Mon. Not. R. Astron. Soc. **278,** 965–974 (1996)

Spectral analysis of the nuclear stellar population and gas emission in NGC 6240

Henrique R. Schmitt,★† Eduardo Bica† and Miriani G. Pastoriza†
Departamento de Astronomia, IF-UFRGS, CP 15051, CEP 91501-970, Porto Alegre, RS, Brasil

Accepted 1995 September 12. Received 1995 April 24; in original form 1994 November 4

ABSTRACT

We analyse the nuclear stellar population and emission-line spectrum in the range $\lambda\lambda$ 3100–9700 Å of the infrared luminous merger galaxy NGC 6240. Two spectral extractions from CCD frames are studied: one corresponding to the double nucleus and the other from a light peak 4 arcsec east of the nucleus. The double nucleus is $\Delta E(B-V) \approx 0.30$ mag more reddened and has a stronger interstellar Na I D absorption as compared to the eastern peak; otherwise the two extractions present similar spectral properties, in particular the dereddened continuum distribution and emission-line ratios. The population synthesis of the double nucleus, which has age and metallicity as free parameters and is based on spectral properties of a library of star clusters, indicates that the continuum flux fraction at 5870 Å owing to an old bulge/halo component is ≈75 per cent, that of intermediate-age components (1 to 5 Gyr) is ≈5 per cent, and that associated with young ones (50 to 500 Myr) is ≈20 per cent. Currently star-forming regions do not contribute more than 1–2 per cent to the continuum at 5870 Å, and this amount is contributed only if they are differentially reddened from the rest of the stellar components by $\Delta E(B-V)_i > 1.00$. The age distribution of the nuclear stellar population, when compared to that found in normal nuclei, sets constraints on the age of the dynamical interaction that led to the present merger; the synthesis suggests that the interaction has been operating for ≈1 Gyr. We derive an internal reddening affecting the nuclear stellar population of $E(B-V)_{sp} = 0.48$. The population-subtracted optical emission-line spectrum is typical of a shock-heated gas. We derive an internal reddening for the emitting gas clouds of $E(B-V)_g = 0.60$. We conclude that in the central 2–3 kpc of NGC 6240 the old (bulge) and 1-Gyr to 50-Myr stellar components are homogeneously mixed, and they coexist with colliding gas clouds from the discs of the merging spirals. The continuum and line emission flux from currently star-forming regions is apparently blocked from the optical spectrum by dust absorption, and their absorbed photons from the ultraviolet to the optical appear to be the source of the strong emission observed with *IRAS*.

Key words: galaxies: individual: NGC 6240 – galaxies: interactions – galaxies: nuclei.

1 INTRODUCTION

NGC 6240 is one of the most luminous infrared galaxies with $L_{IR} = 5.28 \times 10^{11}\ L_{\odot}$ (Wright, Joseph & Meikle 1984; Sanders et al. 1986). The extremely disturbed morphology of this galaxy, with dust lanes, bubbles and plumes, appears to arise from the collision of two spiral galaxies (Fosbury & Wall 1979). Fried & Schulz (1983), using near-IR images, found that NGC 6240 had a double nucleus separated by 1.8 arcsec along the north–south direction, with the brightest component being the southern one. Fried & Ulrich (1985) determined that the two nuclei differ by 148 km s^{-1} in radial velocities, which reinforces the merger idea. Recently Barbieri et al. (1993) presented a near-UV image of

★Present address: Space Telescope Science Institute, 3700 San Martin Drive, Baltimore, MD 21218.
†CNPq fellow.

NGC 6240 taken with the *Hubble ST* Faint Object Camera. They resolved the double nucleus into several compact knots of ≈0.2 arcsec and also observed extended emission. The northern (fainter) component has only one source, while the southern one has several knots.

There are several controversial results about the energy source of this galaxy, which range from shock heated gas to starburst and from LINER-like to Seyfert activity. Rieke et al. (1985) concluded that NGC 6240 had a strong burst of star formation from the spectral characteristics in the ranges 2.1 to 2.4 μm and 3.2 to 3.6 μm, and that this burst explains the far-IR luminosity. They also point out the strong lines from shocked molecular hydrogen. Smith, Aitken & Roche (1989) concluded that the presence of dust emission features at 7.7, 8.6 and 12.5 μm, and the strong silicate absorption at 9.7 μm, are consistent with having a starburst as the major source of luminosity. From higher resolution spectra in the ranges 1.5 to 1.8 μm and 2.0 to 2.5 μm, Lester, Harvey & Carr (1988) concluded that the molecular hydrogen emission in NGC 6240 is shock heated, and that a large fraction of the observed hydrogen recombinaton lines could arise in shocks as well. Kirhakos & Phillips (1989) compared the emission line ratios in the range 5500 to 9950 Å with photoionization and shock models, concluding that the gas in NGC 6240 was being ionized by shocks. The optical spectrum of NGC 6240 has often been classified as a LINER, in particular by the presence of the strong [O I]λ6300 Å (Kirhakos & Phillips 1989). DePoy, Becklin & Wynn-Williams (1986) interpreted their 2.1 to 2.5 μm spectrum of NGC 6240, together with optical and *IRAS* observations, in terms of an active nucleus similar to Seyfert galaxies.

The galaxy has a heliocentric radial velocity of 7340 km s^{-1} which gives, assuming $H_0 = 75$ km s^{-1} Mpc^{-1}, a distance of 98 Mpc and a scale of 475 pc $arcsec^{-1}$, which will be used in this work. Not much information is available about the nature of the nuclear stellar population. The aim of the present study is to explore the nuclear stellar population content in NGC 6240 using optical spectra and the population synthesis method based on star cluster integrated spectra (Bica & Alloin 1986a, 1986b, 1987; hereafter BA86a, BA86b and BA87; Bica 1988). A suitable model for the underlying stellar population is important in order to carry out a population-subtracted emission-line study (Bonatto, Bica & Alloin 1989), since the stellar absorption can affect substantially some fundamental emission lines used for the derivation of reddening, physical and chemical properties.

In Section 2 we present the observations. In Section 3 we compare the spectra of the two spectral extractions deriving a relative reddening, and we present measurements of equivalent widths and continuum points for the double nucleus. In Section 4 we carry out the population synthesis. In Section 5 we subtract the stellar-population-model spectrum from that of the double nucleus and study the resulting emission-line spectrum. The final discussions, concluding remarks and the prospective work are given in Section 6.

2 OBSERVATIONS

The near-ultraviolet observations were obtained in 1989 July, and the visible to near-infrared ones in 1990 May with the European Southern Observatory (ESO) 1.52-m telescope at La Silla, Chile, with a Boller & Chivens spectrograph. For the near-UV, the instrumentation was the front-illuminated coated GEC CCD ESO #14 with 576 × 385 pixels of size 22 × 22 $μm^2$ and ESO grating #8 (193 Å mm^{-1} in first order) with useful spectral range λλ3100–5300 Å; a slit width of 4 arcsec yielded a spectral resolution of ≈16 Å as measured from comparison lamp lines; three exposures of 20 min were taken. For the visible/near-IR, the instrumentation was the RCA SID 503 high-resolution thinned back-side-illuminated CCD ESO #13 1024 × 640 pixels of size 15 × 15 $μm^2$, and ESO grating # 13 (509 Å mm^{-1} in first order) with useful spectral range λλ3800–9700 Å; a slit width of 2 arcsec provided a resolution of ≈19 Å; two exposures of 20 min were taken. In both runs, a long slit was set in the east–west direction with length corresponding to 3.4 arcmin on the sky in the first run, and 3.1 arcmin in the second, ensuring wide regions for background sky subtractions that were free of flux from the galaxy body. We have observed the standard stars EG 274 and Feige 110 in the near-UV run and EG 274, LTT 3218 and LTT 7987 in the visible/near-IR one, all of which were used for flux calibrations and to correct the spectra for atmospheric absorptions (BA87). The reductions were carried out in a standard way in ESO Garching with the IHAP package.

Fig. 1 shows the light profile along the slit, averaged over the wavelength range 4800–5300 Å. The profile has two peaks separated by 4 arcsec (1.9 kpc), the western one being brighter. We have extracted two spectra, taking the minimum between the two peaks as the borderline. The western extraction (9 arcsec along the slit, ≈4.3 kpc) includes light from the double nucleus components A and B. The eastern one (3.5 arcsec along the slit, ≈1.7 kpc) includes part of the structure

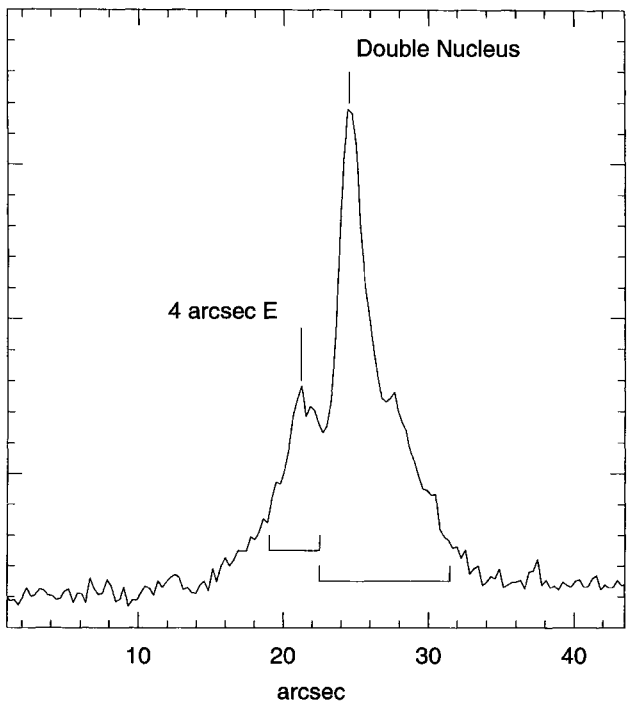

Figure 1. Light profile along the spectrograph slit, averaged over the wavelength range 4800–5300 Å. The position of the extractions are indicated.

C described by Barbieri et al. (1993). The western and eastern extractions are hereafter referred to as double-nucleus and 4-arcsec east regions, respectively.

The calibrated near-UV and visible/near-IR ranges were subsequently linked, averaging the overlapping spectral regions according to their signal-to-noise ratio. The resulting spectra were corrected with a normal reddening law for a foreground reddening of $E(B-V)=0.7$ (Burstein & Heiles 1984). All the subsequent analyses are based on the foreground reddening corrected spectra.

3 COMPARISON OF THE DOUBLE NUCLEUS WITH THE REGION 4 ARCSEC EAST

In Fig. 2 we show the final spectra normalized to the continuum level at 5870 Å. The double-nucleus spectrum has a steeper continuum and a stronger Na I D absorption than that of the 4 arcsec east region, suggesting stronger reddening (Bica & Alloin 1986c, hereafter BA86c), if one assumes that both spectra have similar stellar populations. We also show, in the bottom of Fig. 2, the spectrum of the double nucleus corrected for an internal reddening $\Delta E(B-V)_i=0.30$: the continuum distribution of the two spectra become comparable, which seems to confirm the latter assumption. The equivalent width of the Na I D feature is 4.2 Å in the 4 arcsec east spectrum, whereas that of the double nucleus spectrum amounts to 6.4 Å (see Table 1). The latter value is comparable to those of galaxy nuclei having a strong interstellar gas absorption component in nearly edge-on spirals (BA86c).

We conclude that the columns of interstellar gas and dust, respectively responsible for the Na I D absorption and the reddening, are larger for the double nucleus than for the 4 arcsec east region. We also conclude that the column of interstellar material affecting the double-nucleus region is comparable to that of nearly edge-on spiral galaxies.

Fig. 2 shows that the emission lines, as compared with the continuum, are stronger in the double-nucleus region than in the 4 arcsec east region. Indeed, the equivalent width of the emission lines Hα + [N II] in the 4 arcsec east spectrum is $W_{H\alpha+[N\,II]}=-77$ Å, whereas in the double-nucleus we

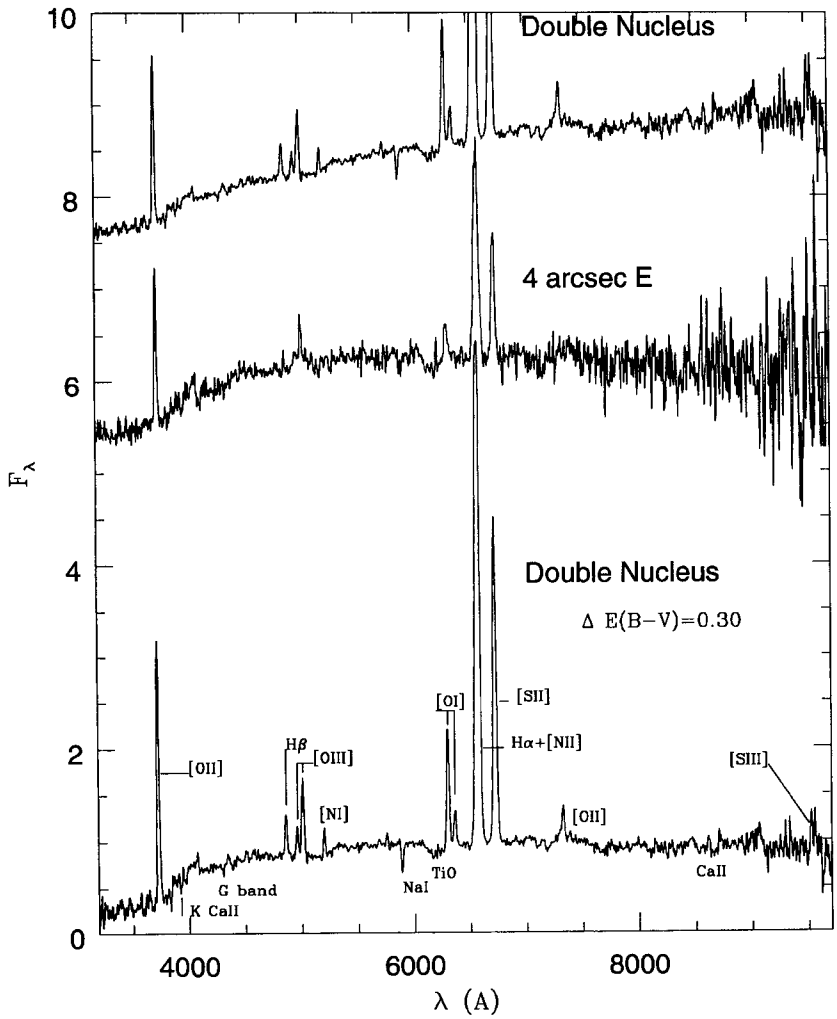

Figure 2. Spectrum of the NGC 6240 double nucleus (top); spectrum of the region 4 arcsec east of the centre (middle). Both are corrected for foreground (Milky Way) reddening of $E(B-V)_f=0.07$. Spectrum of the double nucleus further corrected for an internal reddening difference $\Delta E(B-V)_i=0.30$ (bottom). The spectra are normalized at 5870 Å and are shifted by an additive constant when necessary for clarity.

found $W_{H\alpha+[N\,II]} = -213$ Å (Table 1). Nevertheless, basically the same emission lines are present in both spectra, with similar relative intensities, e.g. a strong [S II]$\lambda\lambda$6717,31 as compared with Hα+[N II], and a moderately strong [O I]λ6300, which suggests that the physical conditions of the emitting gas are similar in both regions. One exception is the Hβ emission line in the 4 arcsec east spectrum, which appears to be much more affected by the absorption from the underlying stellar population.

The nuclear spectrum presents a signal-to-noise ratio suitable for a detailed population synthesis and we present, in Table 1, measurements of equivalent widths and continuum points following the spectral windows and continuum tracings in BA86a, BA87, and also two continuum points in the near-UV as defined by Bica, Alloin & Schmitt (1994).

4 STELLAR POPULATION SYNTHESIS

In order to study the stellar population content of the double nucleus region in NGC 6240, we applied the synthesis method of Bica (1988). This method uses the equivalent widths (W) of the most prominent absorption lines observed in a galaxy, and compares them to those of a model computed from a grid of star cluster Ws for different ages and metallicities (BA86b, BA87). In contrast to population syntheses based on stellar libraries, the star cluster method does not require information on the initial mass function and on surface gravity. Consequently the synthesis is reduced to a two-dimensional problem in the age$\times[Z/Z_{\odot}]$ plane. The search for solutions is carried out through an algorithm that generates combinations of the base components in a given step, and compares the resulting Ws to those of the galaxy; if all the Ws reproduce those of the galaxy, within allowed limits, then it is a possible solution. The algorithm basically consists of a chain of loops, which generates the percentage flux fractions to be attributed to the base elements. The presently used algorithm is a faster version of that in Bica (1988), optimized by the inclusion of several condition tests that avoid the development of combinations for which the sum does not amount to 100 per cent; this version of the algorithm was also employed in the syntheses by Jablonka, Alloin & Bica (1990). The algorithm allows one to estimate the degree of uniqueness of the mean solution by means of the ratio of the number of possible solutions to the total number of combinations. The uniqueness is not as straightforward to estimate in the case of minimization algorithms. The computations were carried out in a UNIX environment with workstations at the Instituto de Física in Porto Alegre.

In the present work, we modified the stellar population synthesis code in order to include, in the search for solutions, continuum ratios to test different values for the internal reddening $E(B-V)_{sp}$ that affects the stellar population. The visible/near-IR continuum ratios for the star clusters are from BA86b (4020 Å/5870 Å and 4570 Å/5870 Å), BA87 (6630 Å/5870 Å, 7520 Å/5870 Å and 8700 Å/5870 Å) and those in the near-UV from Bica, Alloin & Schmitt (1994) (3290 Å/5870 Å and 3660 Å/5870 Å). The code successively dereddens the galaxy input continuum points, and tests them against combinations of those in the base.

An additional modification is the improvement of the spectral properties of the 10-Myr cluster elements in the code, based on the results of the red supergiant phase analysis in LMC and SMC clusters (Bica, Alloin & Santos 1990). The H II-region phase follows that in Bica (1988), i.e. a featureless continuum which acts in the synthesis as a dilutor of absorption lines. In addition to the 10-Myr and H II-region base elements, in which the internal reddening is kept as observed (Bica 1988), we now include in the code 10-Myr and H II-region elements which are differentially reddened with respect to older cluster elements of $\Delta E(B-V)_i = 0.25$, 0.50 and 1.00. These elements can be used to test possible scenarios in galaxies where the star-forming regions are shrouded in dusty environments. We present, in Table 2, the spectral properties of the 10-Myr and H II-region elements as they presently appear in the code matrices of W and continuum points.

The input parameters in the stellar population synthesis of the double nucleus of NGC 6240 were: (i) a path in the age$\times[Z/Z_{\odot}]$ plane which consists of globular cluster age components of different metallicities, in order to represent bulge and halo contributions, together with young and intermediate-age elements of metallicity either equal to, or slightly lower than, that of the most metallic old component (the former type of path could represent a chemical enrichment of the young/intermediate-age components comparable to that attained by the bulge, whereas the latter path could represent star formation with a less metallic gas from outside the galaxy central regions, which is not unexpected in merging galaxies); (ii) the measured equivalent widths of the absorption lines K Ca II, CN, G Band, Ca II 8542 Å and Ca II 8662 Å and Hδ in NGC 6240 (Table 1) and their allowed limits, typically of 1–2 Å; (iii) the continuum ratios presented in Table 1, as well as their allowed limits, typically of 5–10 per cent and (iv) the range and step of $E(B-V)_{sp}$ values to be tested, which we adopted, respectively, as 0 to 1.00 with step 0.02. The W of Mg I was not used because NGC 6240 has a strong [N I] 5200 Å affecting the spectral window;

Table 1. Measurements.

	Windows (Å)	Feature	W_λ (Å)
1	3908–3952	K CaII	6.9±1.5
2	4082–4124	Hδ	4.3±1.0
3	4150–4214	CN	6.4±1.6
4	4284–4318	G band	4.9±1.1
5	4318–4364	Hγ	0.6±1.2
6	4846–4884	Hβ	-10.5±1.2
7	5156–5196	MgI+[NI]	1.5±0.7
8	5880–5914	NaID	6.4±0.7
9	6540–6586	Hα+[NII]	-213±3.0
10	8520–8564	CaII	4.9±1.3
11	8640–8700	CaII	5.3±2.3
	Continua (Å)	Ratios	
a	3290/5870	0.15±0.05	
b	3660/5870	0.24±0.04	
c	4020/5870	0.50±0.04	
d	4570/5870	0.67±0.05	
e	6630/5870	1.15±0.04	
f	7520/5870	1.28±0.04	
g	8700/5870	1.40±0.05	

Table 2. H II-region and 10-Myr elements in the code.

Equivalent Widths

Base Element	KCaII 3933	CN 4200	G 4300	MgI 5175	CaII 8542	CaII 8662	Hδ 4100	Hγ 4340	Hβ 4861
10Myr,[Z/Z⊙]=0.6	2.6	1.4	0.3	2.5	8.2	6.9	4.5	3.5	3.9
10Myr,[Z/Z⊙]=0.3	2.4	1.3	0.3	2.5	7.4	6.3	4.5	3.5	3.9
10Myr,[Z/Z⊙]=0.0	2.2	1.1	0.3	2.0	6.6	5.8	4.5	3.5	3.9
10Myr,[Z/Z⊙]=-0.5	1.9	0.8	0.2	1.5	5.4	4.8	4.5	3.5	3.9
HIIR,0.6≤[Z/Z⊙]≤ −0.3	0.0	0.0	0.0	0.0	0.0	0.0	0.0	0.0	0.0

Continuum points

Base Element	3290 5870	3660 5870	4020 5870	4570 5870	6630 5870	7520 5870	8700 5870
10Myr, E(B–V)=0.00	2.10	1.52	1.45	1.11	0.95	0.99	0.94
10Myr, E(B–V)=0.25	1.27	1.01	1.03	0.88	1.05	1.21	1.26
10Myr, E(B–V)=0.50	0.81	0.67	0.74	0.69	1.15	1.46	1.67
10Myr, E(B–V)=1.00	0.28	0.30	0.37	0.43	1.40	2.16	2.98
HIIR, E(B–V)=0.00	3.78	2.56	2.20	1.73	0.74	0.56	0.37
HIIR, E(B–V)=0.25	2.28	1.70	1.56	1.37	0.82	0.68	0.50
HIIR, E(B–V)=0.50	1.46	1.14	1.11	1.09	0.92	0.82	0.68
HIIR, E(B–V)=1.00	0.50	0.50	0.56	0.49	1.14	1.22	1.28

The continuum points are assumed to be independent of metallicity, since the flux from hot stars is basically dominant in these very young elements.

neither have we used Hβ nor Hγ, because of emission contamination.

We show the results of the stellar population synthesis for NGC 6240 in Table 3. After testing all paths attaining different maximum metallicities, we found that the solution well occurs in the three paths shown in Table 3, together with complementary information on the calculations as indicated in the Table notes. The paths suggest that the bulges of the merging spiral galaxies basically attained a solar or slightly higher metallicity and that the young/intermediate-age components have solar or slightly subsolar metallicity. The values in the paths correspond to percentage continuum flux contributions at 5870 Å for the mean of all solutions found. The dominant stellar population components (≈75 per cent) are in the old-age bin, of which ≈40 per cent have $[Z/Z_\odot] \geq -0.5$, which can be identified as a bulge population, and the rest as bulge/halo intermediate- to metal-poor components. The intermediate-age components (1 to 5 Gyr) basically amount to ≈5 per cent, and the young ones, in the range 50 to 500 Myr, amount to ≈20 per cent. In all cases, a peak occurs at 100 Myr with 11–15 per cent, which indicates that an enhanced star formation event occurred at that epoch, in turn providing clues to the details of the dynamical history of the merger. When compared to the syntheses of normal nuclei dominated by old populations in Bica (1988), the results of Table 3 for NGC 6240 indicate an excess of components with ages as high as 1 Gyr, which might set constraints on how long the two spiral galaxies might have been inducing star formation as a consequence of their gravitational interaction.

The solutions in each path occur only for reddening values affecting the stellar population components at about $E(B-V)_{sp} \approx 0.48$ to 0.51. The information in the Table 3 notes indicates that 352 716 combinations of the base elements were tested for each reddening value; they correspond to all combinations of 12 base elements at a 10 per cent step. Considering that 51 reddening values between $0.00 \leq E(B-V)_{sp} \leq 1.00$ are tested, we end up with a total of 17 988 516 combinations in each path. Typically the computing time for a complete path is one hour. The total number of solutions in each path varies from 240 to 1852 and consequently the ratio of combinations to solutions typically ranges from ≈75 000 to ≈10 000, which corresponds to a high degree of uniqueness. Considering only the combinations corresponding to the reddening peak, typically one solution occurs for every 3296 (path A) or 644 (path C), which is also a non-negligible degree of uniqueness.

Following Bica (1988) we visualize the synthesis results by summing up the closest available spectral templates of star clusters, according to the percentage fluxes for the synthesis components in the paths of Table 3. The templates used were G5 to G1, which are averages of Galactic globular clusters in the range $-2.0 \leq [Z/Z_\odot] \leq 0.0$, I1 and I2 which contain Galactic and LMC intermediate-age star clusters, and Y4 to Y2 which contain Galactic and LMC blue clusters. The model spectrum derived from the solution in path A provided the best results when compared to the NGC 6240 spectrum, since the molecular bands of TiO were stronger than those in the models based on paths B and C, where the proportion of metal-poor to metal-rich components in the old-age bin are enhanced relative to path A. Thus, the path A solution will be adopted in the subsequent discussions. We show, in Fig. 3, the results for path A and the NGC 6240 double-nucleus spectrum corrected for the corresponding

Table 3. Stellar population synthesis results.

Path A

Age:	HIIR	10^7	5×10^7	10^8	5×10^8	10^9	5×10^9	$>10^{10}$	$[Z/Z_\odot]$
									+0.6
									+0.3
								24.2	0.0
	0.0	0.0	0.9	15.7	3.3	2.1	1.7	21.9	−0.5
								11.9	−1.0
								9.9	−1.5
								8.4	−2.0

Path B

Age:	HIIR	10^7	5×10^7	10^8	5×10^8	10^9	5×10^9	$>10^{10}$	$[Z/Z_\odot]$
									+0.6
								11.4	+0.3
	0.0	0.0	1.6	12.3	5.9	2.9	1.7	10.5	0.0
								11.6	−0.5
								11.5	−1.0
								15.0	−1.5
								15.6	−2.0

Path C

Age:	HIIR	10^7	5×10^7	10^8	5×10^8	10^9	5×10^9	$>10^{10}$	$[Z/Z_\odot]$
									+0.6
									+0.3
	0.0	0.0	1.5	11.2	7.0	3.6	2.6	15.2	0.0
								15.4	−0.5
								13.0	−1.0
								15.7	−1.5
								14.8	−2.0

Notes. Path A: testing $0.00 \le E(B-V)_{sp} \le 1.00$ with step 0.02; combinations of elements for each $E(B-V)_{sp}$: 352716; combinations of elements for all $E(B-V)_{sp}$: 17988516; solutions for the $E(B-V)_{sp}$ peak: 107; solutions for all $E(B-V)_{sp}$: 240; mean $E(B-V)_{sp} = 0.48 \pm 0.02$. Path B: testing $0.00 \le E(B-V)_{sp} \le 1.00$ with step 0.02; combinations of elements for each $E(B-V)_{sp}$: 352716; combinations of elements for all $E(B-V)_{sp}$: 17988516; solutions for the $E(B-V)_{sp}$ peak: 548; solutions for all $E(B-V)_{sp}$: 1852; mean $E(B-V)_{sp} = 0.50 \pm 0.03$. Path C: testing $0.00 \le E(B-V)_{sp} \le 1.00$ with step 0.02; combinations of elements for each $E(B-V)_{sp}$: 352716; combinations of elements for all $E(B-V)_{sp}$: 17988516; solutions for the $E(B-V)_{sp}$ peak: 170; solutions for all $E(B-V)_{sp}$: 653; mean $E(B-V)_{sp} = 0.51 \pm 0.03$.

stellar population reddening $E(B-V)_{sp} = 0.48$, together with the contributions of different components summed into groups. A good agreement is seen for the spectral distibutions of the model and of the galaxy. The importance of the absorption component in the emission line Hβ is noticeable. In the stellar population synthesis we find $W(H\beta) = 4.6$ Å, whereas in the observed spectrum $W(H\beta) = -10.5$ Å, showing that ≈ 30 per cent of the Hβ flux in emission is absorbed, an amount that cannot be neglected in the determination of the gas reddening by the Balmer decrement. The Na I D equivalent width of the model spectrum is 2.7 Å, which, when compared to the observed value (Table 1), implies an interstellar component of $\Delta W(\text{Na I D}) = 3.7$ Å, comparable to the highest values observed in nearly edge-on galaxies (BA86c).

It is noteworthy that, in the solutions of Table 3, no contribution from the H II region or the 10-Myr components appears. This can be understood by the comparison of the NGC 6240 spectrum (corrected for the stellar population reddening) with the continuum distributions of the H II region and of the 10-Myr components, shown to scale for a 10 per cent continuum contribution at 5870 Å in Fig. 4 (lower panel). The H II-region continuum and the 10-Myr component are too blue in the near-UV to provide any contribution to the galaxy spectrum. They might become possible contributors if they were differentially greatly reddened with respect to the older population components, as suggested in Fig. 4 (upper panel). Nevertheless, H II-region and 10-Myr components, differentially reddened by $\Delta E(B-V)_i = 0$, 0.25, 0.50 and 1.00, were used in the

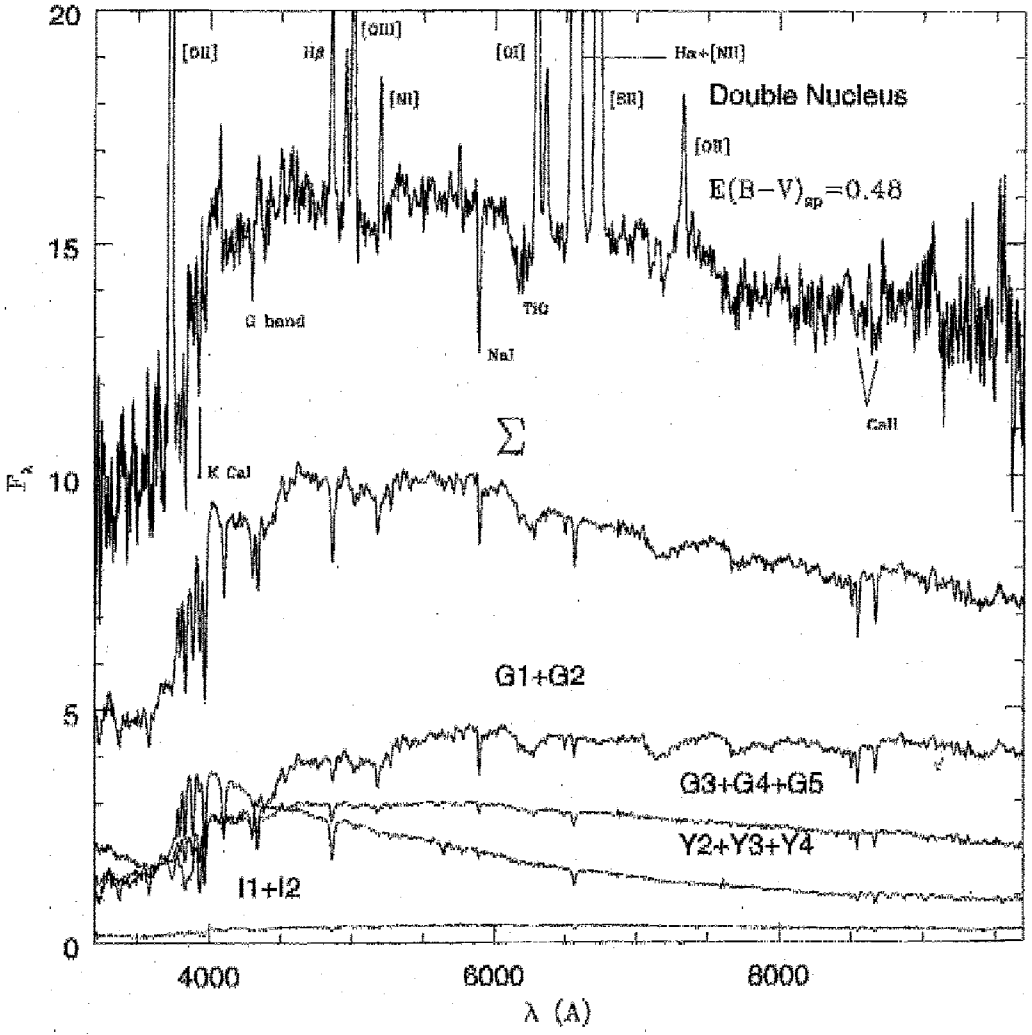

Figure 3. Spectrum of the NGC 6240 double nucleus corrected for foreground reddening $E(B-V)_f=0.07$, and that affecting the stellar population $E(B-V)_{sp}=0.48$ (top). Result of the stellar population synthesis in Path A (middle). Components of the synthesis (bottom) grouped into old metal rich (G1 + G2), old metal poor (G3 + G4 + G5), intermediate age (I2 + I1) and young (Y4 + Y3 + Y2), shown to scale according to their flux fraction contributions at 5870 Å.

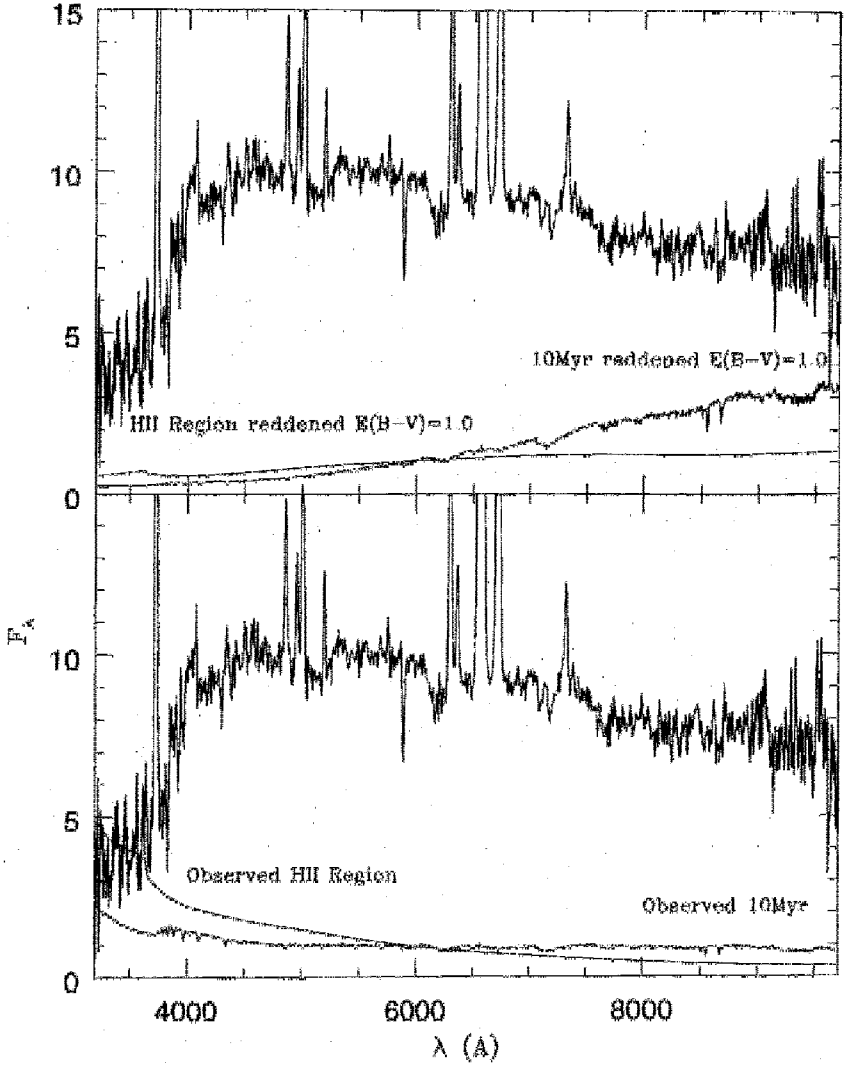

Figure 4. The double nucleus spectrum corrected for $E(B-V)_f$ and $E(B-V)_{sp}$ compared to the H II region and the 10-Myr cluster templates, which are shown as observed (lower panel) and differentially reddened by $\Delta E(B-V)_s=1.00$ (upper panel). The templates are scaled to a 10 per cent flux contribution at 5870 Å relative to the galaxy spectrum.

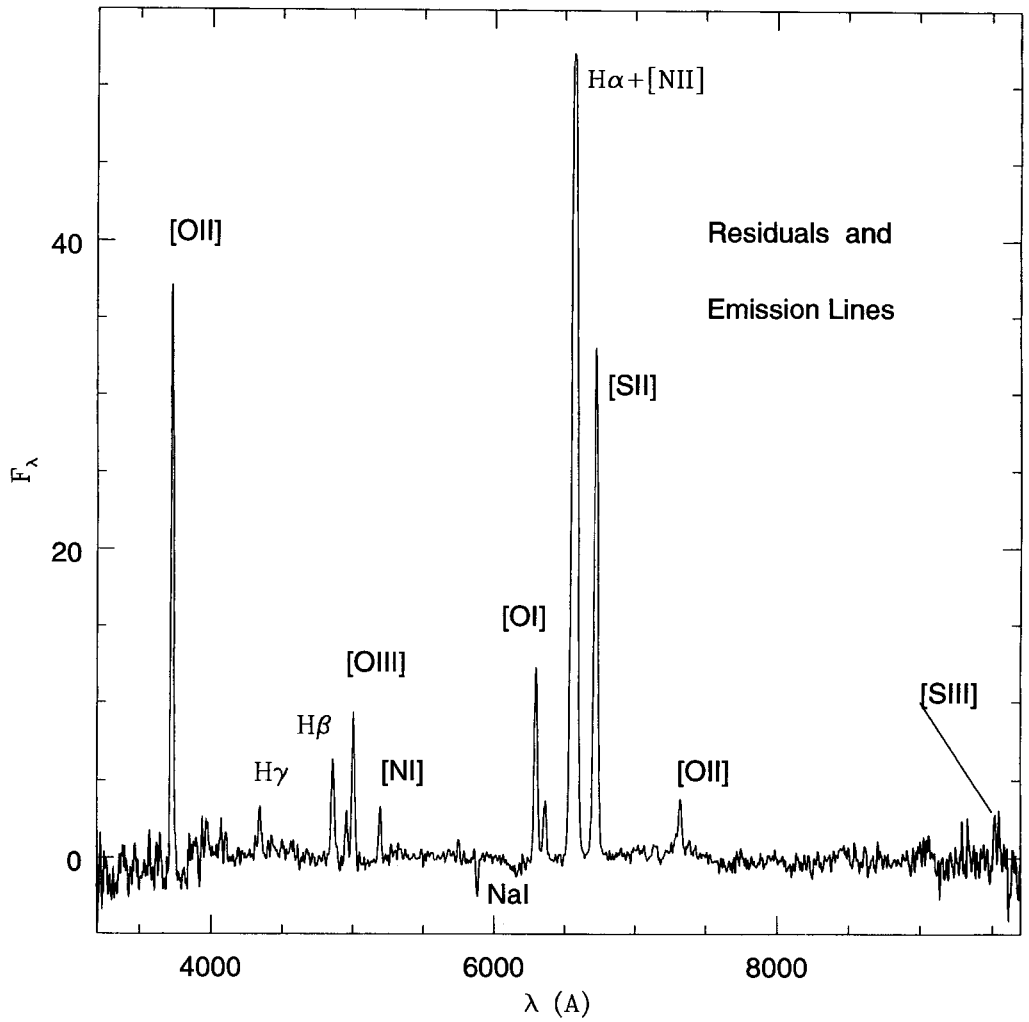

Figure 5. Subtraction of the synthetic spectrum from that of NGC 6240 in Fig. 3, showing the residuals and providing the emission-line spectrum for the subsequent analyses. This emission-line spectrum results corrected for the foreground (Milky Way) reddening $E(B-V)_f = 0.07$, and for that affecting the stellar population $E(B-V)_{sp} = 0.48$.

computations that led to the solutions in Table 3 and null contributions resulted in all cases. The latter computations used a 10 per cent step for the contributions of base elements. In spite of the fact that the computing time increased considerably, we ran some paths with a 5 per cent step in order to check whether the step was influencing the results. The mean solutions in path A indicated the appearance of H II-region contribution in the range 1–2 per cent only for the differentially reddened component $\Delta E(B-V)_i = 1.00$. We thus conclude that currently star-forming regions can only contribute 1–2 per cent to the flux at $\lambda 5870$ Å of the emergent optical spectrum of the central parts of NGC 6240, if they are differentially reddened with respect to the rest of the stellar population components by $\Delta E(B-V)_i \geq 1.00$.

5 ANALYSIS OF THE EMISSION-LINES

We show in Fig. 5 the subtraction of the model spectrum from that of the double nucleus corrected for $E(B-V)_{sp} = 0.48$ (see Fig. 3). This stellar-population-subtracted spectrum is used to study the emission lines. The emission lines were fitted with Gaussians in order to measure their fluxes, which are shown in Table 4, relative to that of Hβ normalized at 1.0. We also show errors estimated from the noise in each region, and the uncertainty in the continuum definition. We used the theoretical ratio [N II]$\lambda 6584$/[N II]$\lambda 6548 = 2.97$ and assumed that they had equal FWHM in the deblending procedure with Hα. The deblending of these important lines was straightforward, and the estimated errors are similar to those of isolated lines (Table 4).

As a consequence of the procedures applied to the spectra in Section 4, the emission-line ratios in column 3 of Table 4 are shown corrected for the foreground reddening $[E(B-V)_f = 0.07]$ and for that affecting the stellar population $[E(B-V)_{sp} = 0.48]$. The values shown in column 4 were further corrected for the gas reddening $E(B-V)_{gas} = 0.60$. The latter value was calculated assuming case B recombination and the intrinsic value Hα/H$\beta = 2.87$ (Osterbrock 1989). Notice that the resulting Hγ/Hβ (column 4) is 0.43, which is basically comparable to the expected value 0.47, within uncertainties.

Table 4. Emission-line fluxes relative to Hβ.

Line	Wavelength(Å)	$F_\lambda^{E(B-V)_{sp}=0.48}$	$F_\lambda^{E(B-V)_{gas}=0.60}$
[OII]	3727	4.48±0.67	7.61±1.14
[SII]	4068+4076	0.17±0.1	0.25±0.15
Hγ	4340	0.32±0.08	0.43±0.09
Hβ	4861	1.00±0.07	1.00±0.07
[OIII]	4959	0.48±0.09	0.45±0.08
[OIII]	5007	1.42±0.1	1.35±0.09
[NI]	5200	0.37±0.07	0.33
[NII]	5755	0.13±0.07	0.09±0.05
[OI]	6300	1.82±0.18	1.04±0.1
[OI]	6363	0.58±0.12	0.33±0.07
[NII]	6548	2.02±0.1	1.07±0.05
Hα	6563	5.46±0.27	2.87±0.14
[NII]	6584	6.02±0.3	3.17±0.16
[SII]	6717+6731	5.79±0.29	3.05±0.15
[OII]	7324	0.51±0.1	0.22±0.04
[SIII]	9069	—	0.035[a]
[SIII]	9532	0.30±0.1	0.09±0.03

Note: the third column corresponds to the line fluxes corrected for the stellar population reddening, while the fourth column includes an additional correction internal to the gas based on Hα/Hβ=2.87.

[a]This value was estimated using that of [S III]λ9532 Å and the transition probabilities from Osterbrock (1989).

In order to study the ionizing mechanism of NGC 6240, we compared emission-line ratios, calculated from column 4 of Table 4, with the diagnostic diagrams [N II]λ6584/Hα × [O II]λ3727/[O III]λ5007, and [N II]λ6584/Hα × [O III]λ5007/Hβ from Baldwin, Phillips & Terlevich (1981). Considering the errors in the fluxes of the emission lines (Table 4) and the sensitivity of [O II]λ3727/[O III]λ5007 on reddening uncertainties, in all cases the points were located in the loci of shock heated objects. We also compared the observations with the diagnostic diagrams [S II]$\lambda\lambda$6717,31/Hα × [S III] $\lambda\lambda$9069,9532/Hα and [S II] $\lambda\lambda$6717,31 [S III]$\lambda\lambda$9069,9532 × [O II]λ3727/[O III]$\lambda\lambda$4959,5007 from Díaz, Pagel & Wilson (1985) (see also Bonatto et al. 1989, Kirhakos & Phillips 1989). Shock models from Shull & McKee (1979) are included in those diagrams. The points of NGC 6240 are located, within uncertainties, around a sequence of models which indicates that the gas is being heated by shocks with velocities in the range 90–100 km s^{-1}. In order to leave the locus of shocks in the former diagram, it would be necessary to have much stronger [S III]$\lambda\lambda$9069, 9532 lines, of the same order as the [S II]$\lambda\lambda$6717,31 lines; any additional reddening correction would further decrease the relative intensity of the [S III] lines. The emisson-line spectrum of NGC 6240 shows the presence of prominent low-ionization lines such as [O I]$\lambda\lambda$6300,6363 Å and [N I]λ5200 Å, which are also enhanced in shock models and observed supernova remnants (SNRs) (Dopita et al. 1984).

6 DISCUSSION AND CONCLUDING REMARKS

From the stellar population analysis in Section 4, and that of the population-subtracted emission-line spectrum in Section 5, together with results from other studies in the literature (Section 1), it is possible to constrain a physical scenario to explain the emergent optical flux from the central regions of NGC 6240.

The dominant stellar population in the optical is very old, arising mostly from the metal-rich bulges of the merging spiral galaxies, and also from a metal-poor bulge and/or halo component. An important blue stellar population component with age ≈100 Myr is detected, which might be a burst of star formation, associated to a close encounter of the galaxies during the dynamical history of the merger. In the stellar population synthesis of the central parts of NGC 6240, when compared to normal bulges dominated by old populations (Bica 1988), we detected an excess of components with ages less than ≈1 Gyr, which set an upper limit to the age of the dynamical interaction between the two spiral galaxies. Using $A_V/E(B-V)=3.1$, the average internal reddening affecting the stellar populations in the double nucleus of NGC 6240 is $A_{V_{sp}}=1.49$. The population-subtracted emission-line spectrum indicates, from the Balmer decrement, that the emitting clouds have an additional reddening $A_{V_g}=1.86$. The mechanism responsible for the gas ionization appears to be shock heating, probably arising from colliding clouds from the inner discs of the two spirals. The 4-arcsec east region spectrum suggests that the stellar population and the emitting gas have characteristics similar to those of the double-nucleus region, except that the stellar population (and the emitting gas) is less reddened by $\Delta A_{V_{sp}}\approx 0.93$ in the former. Consequently, bulge stars and young/intermediate-age stars formed during the merger and/or pre-existing in the central discs appear to be homogeneously mixed to distances as far as 2 kpc from the centre of the galaxy. Currently, star-forming regions cannot contribute to the stellar population continuum at 5870 Å by more than 1–2 per cent, and this is possible only if they are differentially reddened relative to the rest of the stellar components by $\Delta A_{V_i}>3.1$, or total $A_{V_i}>4.8$ considering also that affecting the overall stellar population and the foreground reddening. On the other hand, the currently star-forming regions may show up directly in the infrared, owing to the weaker absorption. Evidence of this was found by Rieke et al. (1985); absorbed flux from the ultraviolet, up to as far as the optical region, would consequently explain the strong emission observed with *IRAS* in this galaxy (Sanders et al. 1986) as heated dust. These conclusions remain basically the same if one is dealing with an AGN (DePoy et al. 1986). However, neither a star-forming complex nor an active nucleus appear to be contributing significantly to the ionization of the gas, as observed from optical emission lines.

As prospective work in stellar populations and gas emission, spatially resolved spectra throughout the body of NGC 6240 are desirable in order to understand in detail the distribution and mixtures of stellar population components and gas clouds, which in turn would provide more insight on merging processes.

ACKNOWLEDGMENTS

This work was partially supported by the Brazilian institutions CNPq and FINEP.

REFERENCES

Baldwin J. A., Phillips M. M., Terlevich R., 1981, PASP, 93, 5
Barbieri C. et al. 1993, A&A, 273, 1
Bica E., 1988, A&A, 195, 76
Bica E., Alloin D., 1986a, A&A, 162, 21 (BA86a)
Bica E., Alloin D., 1986b, A&AS, 66, 171 (BA86b)
Bica E., Alloin D., 1986c, A&A, 166, 83 (BA96c)
Bica E., Alloin D., 1987, A&A, 186, 49
Bica E., Alloin D., Santos J. F. C., Jr, A&A, 235, 103
Bica E., Alloin D., Schmitt H. R., 1994, A&A, 283, 805
Bonatto Ch., Bica E., Alloin D., 1989, A&A, 226, 23
Burstein D., Heiles C., 1984, ApJS, 54, 33
DePoy D. L., Becklin E. E., Wynn-Williams C. G., 1986, ApJ, 307, 116
Díaz A. I., Pagel B. E. J., Wilson I. R. G., 1985, MNRAS, 212, 737
Dopita M. A., Binette L., D'Odorico S., Benvenuti P., 1984, ApJ, 276, 653
Fosbury R. A. E., Wall J. V., 1979, MNRAS, 189, 79
Fried J. M., Schulz H., 1983, A&A, 118, 166
Fried J. W., Ulrich H., 1985, A&A, 152, L14
Jablonka P., Alloin D., Bica E., 1990, A&A, 235, 22
Kirhakos S., Phillips M. M., 1989, PASP, 101, 949
Lester D. F., Harvey P. M., Carr J., 1988, ApJ, 329, 641
Osterbrock D. E., 1989, Astrophysics of Gaseous Nebulae and Active Galactic Nuclei. University Science Books, Mill Valley, California
Rieke G. H., Cutri R. M., Black J. H., Kailey W. F., McAlaray C. W., Lebofsky M. J., Elston R., 1985, ApJ, 290, 116
Sanders D. B., Scoville N. Z., Young J. S., Soifer B. T., Schloerb F. P., Rice W. L., Danielson G. E., 1986, ApJ, 305, 830
Shull J. M., McKee C. E., 1979, ApJ, 227, 131
Smith C. H., Aitken D. K., Roche P. F., 1989, MNRAS, 241, 425
Wright G. S., Joseph R. D., Meikle W. P. S., 1984, Nat, 309, 430